





Regulation of the *THRA* gene, encoding the thyroid hormone nuclear receptor TR α 1, in intestinal lesions

Maria Virginia Giolito^{1,2} , Théo La Rosa^{2,†}, Diana Farhat^{1,2} , Serguei Bodoirat¹, Gabriela D. A. Guardia³, Claire Domon-Dell¹, Pedro A. F. Galante³, Jean-Noel Freund¹  and Michelina Plateroti^{1,2} 

1 Inserm, IRFAC/UMR-S1113, FMTS, Université de Strasbourg, France

2 INSERM U1052, CNRS UMR5286, Centre de Recherche en Cancérologie de Lyon, France

3 Centro de Oncologia Molecular, Hospital Sírio-Libanês, São Paulo, Brazil

Keywords

colon cancer; intestinal organoids; THRA; thyroid hormone nuclear receptor; TR α 1

Correspondence

M. Plateroti, INSERM U1113, 3 avenue Molière, 67200 Strasbourg, France
Tel: +33 3 88 27 53 56
E-mail: plateroti@unistra.fr

Present address

[†]Stem-Cell and Brain Research Institute, U1208 INSERM, USC1361 INRA, Bron, France

(Received 16 October 2021, revised 5 July 2022, accepted 29 July 2022, available online 10 October 2022)

doi:10.1002/1878-0261.13298

The *THRA* gene, encoding the thyroid hormone nuclear receptor TR α 1, is expressed in an increasing gradient at the bottom of intestinal crypts, overlapping with high Wnt and Notch activities. Importantly, *THRA* is upregulated in colorectal cancers, particularly in the high-Wnt molecular subtype. The basis of this specific and/or altered expression pattern has remained unknown. To define the mechanisms controlling *THRA* transcription and TR α 1 expression, we used multiple *in vitro* and *ex vivo* approaches. Promoter analysis demonstrated that transcription factors important for crypt homeostasis and altered in colorectal cancers, such as transcription factor 7-like 2 (TCF7L2; Wnt pathway), recombining binding protein suppressor of hairless (RBPJ; Notch pathway), and homeobox protein CDX2 (epithelial cell identity), modulate *THRA* activity. Specifically, although TCF7L2 and CDX2 stimulated *THRA*, RBPJ induced its repression. In-depth analysis of the Wnt-dependent increase showed direct regulation of the *THRA* promoter in cells and of TR α 1 expression in murine enteroids. Given our previous results on the control of the Wnt pathway by TR α 1, our new results unveil a complex regulatory loop and synergy between these endocrine and epithelial-cell-intrinsic signals. Our work describes, for the first time, the regulation of the *THRA* gene in specific cell and tumor contexts.

1. Introduction

The thyroid hormone (TH) nuclear receptor TRs are T3-modulated transcription factors belonging to the nuclear hormone receptor protein superfamily [1]. THs and TRs are involved in multiple processes in organism development, physiology, and, eventually, pathological events [2–5]. From a molecular point of view, they modulate the expression of target genes by binding to thyroid hormone response elements (TREs)

present in regulatory regions of target genes. Upon T3 binding, TRs undergo conformational modification, resulting in activation or repression of the transcriptional machinery [2].

One well-defined organ target of THs and the receptor TR α 1 is the intestine. Indeed, the involvement of TR α 1-dependent signaling and/or TH status has been reported in the normal intestine [6–9] and in intestinal tumor biology [6,7,10–12]. Studies in *Thra*- and *Thrb*-knockout animals showed that TR α 1 is responsible for

Abbreviations

CMS, consensus molecular subtype; CRC, colorectal cancer; IHC, immunohistochemistry; KO, knock-out; qPCR, quantitative polymerase chain reaction; RLU, relative luciferase units; RT, retro transcription; SC, stem cell; TH, thyroid hormone; THRA, thyroid hormone receptor alpha gene; TMA, tissue microarray analysis; TR, thyroid hormone receptor; WB, western blot.

TH signaling in intestinal crypts, where it controls the biology of stem cells (SCs) and their fate [13], as well as the balance between cell proliferation and cell differentiation through its actions on the Wnt and Notch pathways (rev in Refs [6,7,10]). In accordance with this important role, overexpression of TR α 1 in the intestinal epithelium (*vil*-TR α 1 mice) in a mutated-Apc background (*vil*-TR α 1/Apc^{+/-1638N} mice) is responsible for the acceleration of tumor appearance, progression, and aggressiveness compared with Apc-only mutants [14]. Conversely, *Thra* gene loss in the same mutated-Apc background diminishes and slows tumor appearance [15]. Interestingly, the relevance of these observations has been demonstrated in clinics, given that the *THRA* gene and the TR α 1 isoform are frequently overexpressed in human colorectal cancer (CRC) patients [15].

CRC is the third leading cause of cancer death in the world [16]. CRC development is a multistep process triggered by the accumulation of mutations in oncogenes and tumor suppressors, which, in turn, are responsible for tumor initiation and progression [17]. Crypt hyperplasia, hypertrophy, and stem cell (SC) transformation represent very early events in intestinal tumor development [18–20] and depend on alterations of genes in the Wnt and Notch pathways [21,22]. It is worth noting that these cellular and molecular processes are also affected by TR α 1, which synergizes with the Wnt pathway to accelerate neoplastic events [14,15]. Moreover, the expression of the *THRA* gene is upregulated in CRC consensus molecular subtypes (CMS) compared to the normal colon, with significantly higher overexpression in CMS2 [15], which is characterized by high Wnt and Myc signaling activation [23]. However, no information is available on the molecular mechanisms involved in *THRA* regulation in the context of CRC.

Interestingly, the *THRA* gene was characterized in the early 1990s as the cellular homolog of the avian retroviral erythroblastoma virus *v-erbA*, which is involved in neoplastic transformation leading to acute erythroleukemia and sarcomas [24,25], thus suggesting its link with malignancies. However, very few studies have analyzed the genomic organization and transcriptional control of the *THRA* gene [26,27]. Ishida et al. [28] observed that the 615-bp 5'-flanking sequence of the *THRA* promoter presented putative binding sites for several transcription factors, including SP1, cAMP-responsive elements (CRE), CREB, AP1, Krow-20, COUP-TF/EAR-3, and retinoid X receptor (RXR) [28]. Another study described the regulation of the *THRA* gene promoter by the orphan nuclear receptor ERR α [29]. However, these reports did not consider

cell type-specific control under physiological or pathological conditions.

In the current study, we investigated the mechanisms underlying *THRA* transcriptional regulation, including the modulation of the TR α 1 receptor. *In silico* and molecular approaches identified promoter regions and transcription factors important for *THRA* activity. We demonstrated the presence of binding sites for transcription factors involved in intestinal homeostasis and SC/cancer SC biology that are also altered in CRC [30–32], such as TCF7L2 (Wnt pathway) [33], RBPJ (Notch pathway) [34], and CDX2 (intestinal epithelial cell identity) [35]. Finally, in-depth analysis of the Wnt pathway allowed us to recapitulate the regulation of *THRA* transcription and TR α 1 expression by this signaling pathway in human adenocarcinoma cell lines as well as mouse enteroids. This study presents the first extended analysis of *THRA* regulation and its relevance in a patho-physiological context. In addition, it describes, for the first time, the existence of a reciprocal regulatory loop between TR α 1-dependent and Wnt-dependent signals in intestinal epithelial cells.

2. Materials and methods

2.1. Tissue microarray analysis (TMA)

TR α 1 expression has been analyzed by immunohistochemistry on Tissue Focus Colon Cancer Tissue MicroArray, FFPE, 42 × 1 mm cores (CT565864; CliniSciences, Nanterres, France). The TMA was composed of 33 tumors at different stages and 9 normal tissues. The study and label scoring were conducted by the Research Pathology Platform (Lyon, France). Briefly, after deparaffinization and dehydration, tissue sections were heated for 50 min at 97 °C in 10 mM citrate buffer, pH 6.0. To block endogenous peroxidases, tissue sections were incubated in 5% hydrogen peroxide solution. Immunohistochemistry (IHC) was performed on an automated immunostainer (Ventana Discovery XT; Roche, Meylan, France) using an Omnimap DAB Kit (Ventana Medical Systems, Tucson, AZ, USA) according to the manufacturer's instructions. Sections were incubated with the anti-TR α 1 antibody (ab53729, dilution 1 : 50). The secondary anti-rabbit-HRP antibody was applied to the sections, and staining was visualized with DAB solution with 3,3'-diaminobenzidine as a chromogenic substrate. Finally, the sections were counterstained with Gill's hematoxylin and then scanned with a Panoramic Scan II (3D Histech, Budapest, Hungary) at 20×. The scoring of TR α 1 levels (–, negative; +/-, low; + positive; ++, highly positive) was performed independently by two individuals.

2.2. Bioinformatics analyses of the TCGA CRC cohort

To analyze the expression levels of THRA in the TCGA cohort, RNA sequencing data from 270 colon adenocarcinoma (COAD) and 41 adjacent normal samples were obtained from the TCGA data portal (<https://portal.gdc.cancer.gov/>). To obtain Transcripts Per Million (TPM) normalized expression levels of the THRA canonical transcript, we used Kallisto [36] with GENCODE (<https://www.encodegenes.org/>; v29) as reference to the human transcriptome. TCGA samples were also classified according to CMSs [23] using the R package CMS classifier (v1.0.0). Boxplots were created using the R packages ggplot2 (v3.3.2) and ggpubr (v0.4.0), and comparisons between groups were assessed by Wilcoxon tests.

2.3. In silico THRA promoter analysis

Analysis of approximately 3500 bp of the THRA promoter region upstream the transcription start site (TSS) was performed by the MatInspector library (Genomatix, Munich, Germany), using Matrix Family Library Version 11.0. Filters were applied to select a core matrix similarity > 0.85 (85% of conserved homology) using the module General Core Promoter Elements (Optimized).

2.4. Construction of the THRA-luciferase vectors

3238-bp upstream of the transcription starting site of the THRA gene were cloned into the pGL3 basic vector (Promega, Charbonniere-les-Bains, France) to construct the pGL3-THRA-Luc vector (named pGL3-THRA) using MluI (5') and XhoI (3') sites (Fig. S1A). A CT>GC mutation was introduced at positions 816 and 2270 of the pGL3-THRA-luc vector, separately, to mutate the TCF7L2-binding sites and generate the THRA-mut-Luc1 and THRA-mut-Luc2 vectors (named pGL3-THRA-mut-TCF7L2-1 and pGL3-THRA-mut-TCF7L2-2, respectively) (Fig. S1B,C). For the generation of the double mutant vector (named pGL3-THRA-mut-TCF7L2-sites, Fig. S1D), both mutant plasmids were digested with AvrII and StuI enzymes (New England Biolabs, Evry, France). The fragment containing the mutant TCF7L2-1 site was ligated into the vector containing the mutant TCF7L2-2 site using DNA quick ligase (M2200L; New England Biolabs). The ligated mix was used to transform competent bacteria, and the colonies were recovered for DNA plasmid preparation and sequencing. Gene synthesis, site-directed mutagenesis, and sequencing were performed by Eurofins Genomics (Ebersberg, Germany).

2.5. Cell lines and transfection experiments

The human adenocarcinoma cell lines Caco2, HCT116, and SW480 (from ATCC, Rockville, USA) were cultured in DMEM Glutamax (4.5 g·L⁻¹ D-Glucose with pyruvate) medium (ThermoFisher Scientific, Courtaboeuf, France) supplemented with 10% heat-inactivated FBS and 1% penicillin/streptomycin (P/S) (ThermoFisher Scientific) at 37 °C in a humidified atmosphere containing 5% CO₂.

For luciferase assays, we seeded each cell line onto 24-well plates (75 000 cells/well) in DMEM supplemented with 10% FBS and 1% P/S. The next day, we transfected the plasmids using PEI Prime™ linear polyethylenimine (Sigma-Aldrich 919012; Saint-Quentin Fallavier, France) at a ratio of 1 µg DNA/1.5 µL of PEI at 1 mg·mL⁻¹. Transfection was performed for 6 h in culture medium without serum. Luciferase activity was measured 48 h after transfection using the Dual-Luciferase Reporter Assay System (Promega). Data represent the normalized beetle-luciferase/renilla-luciferase activities measured in each well to correct for eventual differences in transfection efficiency from well to well. Experiments were performed at least two times with *n* = 6 for each condition.

2.5.1. Luciferase reporter vectors

THRA-Luc (200 ng/well), THRA-mut1-Luc, THRA-mut2-luc and THRA-dmut-luc (200 ng/well), TopFlash (200 ng/well; Fisher Scientific, Illkirch, France), RBPJ-Luc (200 ng/well, [37]), hLI-Luc (200 ng/well), pGL3-basic (200 ng/well), and pRL-CMV (10 ng/well; Promega) were used. The generation of hLI-Luc was based on a previous publication [38] and consisted of cloning approximately 1 kb of the human LI-cadherin gene promoter into the pGL3 basic vector using SacI (5') and HindIII (3') restriction sites.

2.5.2. Expression vectors

β-Catenin ΔN (100 ng per well, gift from Pr M. Waterman), TCF1E-EVR2 (100 ng per well) [39], TCF1E-EVR2-DN (300 ng per well) [39], CDX2 (100 ng per well) [40], and NICD (100 ng per well) [37] were used. The amounts of DNA under each condition were normalized by adding the empty pBSK vector. The experiments based on Wnt blocking and restimulation were performed by transfecting the TCF1-DN vector (dominant negative; 300 ng per well) in the absence or presence of increasing amounts of β-catenin ΔN expression vector (from 50 to 500 ng per well).

2.5.3. siRNA approach

For CDX2 expression modulation by the siRNA approach, we seeded each cell line into 24-well plates (75 000 cells per well) in DMEM supplemented with 10% FBS and 1% P/S. The next day, we removed the medium and added siRNA CDX2 (Silencer[®] Select siRNA@CDX2 s2876; ThermoFischer) or the siRNA control (Silencer[™] Select Negative Control No. 2 siRNA; ThermoFischer, #4390846) at a final concentration of 10 nM in a mix containing OPTIMEM medium (ThermoFisher Scientific) and lipofectamine RNAiMAX (ThermoFisher Scientific) for 24 h. In CDX2-KD and control cells, we performed *THRA*-luc transfection assays as indicated above.

2.5.4. Treatments with small molecules

For modulation of the Wnt pathway, we used an approach consisting of treatment with small molecules. Transfected cells, as described above were treated with each molecule 24 h before the end of transfection. We used the Wnt agonists CHIR99021, 3 μ M (Sigma-Aldrich) [41] and the Wnt antagonist IWP4, 5 μ M (Tocris, Noyal Chatillon sur Seiche, France) [42]; the Notch agonist Yhhu3792, 2.5 μ M (Tocris) [43]; and the Notch antagonists LY411575, 1 μ M (Sigma-Aldrich, Saint-Quentin-Fallavier, France) [44], and DAPT, 10 μ M (Tocris) [45]. The effect of the Wnt agonist and antagonist on endogenous TR α 1 expression was analyzed by treating the cells for 48 h before harvesting.

2.6. ChIP and qPCR analysis

For ChIP experiments, each cell line was seeded in 6 cm dishes, and the cells recovered after 2 days of culture. Chromatin crosslinking was performed with 1% (vol/vol) formaldehyde for 10 min at room temperature and quenched with 0.125 mol·L⁻¹ glycine for 5 min. ChIP experiments were performed using the EZ-Magna ChIP G Chromatin Immunoprecipitation kit (Sigma-Aldrich, #17-409) as recommended by the supplier. Sonicated chromatin (BioruptorPlus, Diagenod apparatus, Seraing, Belgium; 12 cycles of 30 s ON/30 s OFF on high mode) from 2 \times 10⁶ cells was incubated overnight at 4 °C with 4 μ g of mouse anti- β -catenin antibody (clone 14; BD Transduction Lab, Le Pont de Claix, France) or with immunoglobulin G (IgG) (Cell Signaling, Leiden, The Netherlands). DNA was quantitated by qPCR using SYBR qPCR Premix Ex Taq II (Tli RNaseH Plus; Takara, Saint-Germain-en-Laye, France) in a CFX Connect apparatus (Bio-Rad, Marnes-la-Coquette, France). The primers used

for AXIN2, MYC, THRA-1, THRA-2, PPIB, and HPRT are listed in Table S1. The antibodies are listed in Table S2. Histograms represent the fold enrichment of specific β -catenin DNA binding normalized to the input and compared with the IgG condition (= 1).

2.7. Western blot

Protein samples from each cell line (30 μ g per lane) were prepared with RIPA buffer as described in [15], separated by SDS/PAGE, and transferred to 0.2- μ m PVDF membranes (Bio-Rad). Membranes were blocked with PBS-Tween supplemented with 5% nonfat milk before incubation with primary antibodies. This step was followed by incubation with HRP-conjugated secondary antibodies (Promega). The signal was analyzed using an enzymatic Clarity Substrate Detection Kit and Clarity Max ECL (Bio-Rad) according to the manufacturer's protocol, and image detection was performed using a Pixie imaging system (Gene-sys, France). The antibodies are listed in Table S2.

2.8. Animals, isolation of small intestinal crypts, and enteroid cultures

Villin-Cre^{ERT2} and Apc^{+fl} mice have been bred in our laboratory since 2009, when they were provided by the Institut Curie (Paris, France) [46,47]. For our study, adult 2–4-month-old Apc^{+fl}/Villin-Cre^{ERT2} and Apc^{+fl} mice were maintained in a C57BL/6J genetic background and housed in the same animal facility, where they received standard mouse chow and water *ad libitum*. All experiments were performed in compliance with the French and European guidelines for experimental animal studies and approved by the local committees “Comités d'Éthique Ceccapp” (C2EA55) “the Ministère de l'Enseignement Supérieur et de la Recherche, Direction Générale pour la Recherche et l'Innovation, Secrétariat “Autorisation de projet” (agreement # 13313-2017020210367606).

After sacrifice, we collected the small intestine (from the proximal jejunum to the distal ileum) for crypt preparation and enteroid cultures, using the protocol previously described [13]. Organoids were cultured at 37 °C and 5% CO₂ in IntestiCult Organoid Growth Medium (Stem Cell Technologies, Saint Egreve, France). The medium was changed every 3 days, and organoids were replicated approximately 7 days after the beginning of the culture. For all experiments (three independent experiments from three independent mice), we used organoids after the first replication (R1). Briefly, Matrigel-embedded organoids were grossly dissociated with a micropipette, fragments were washed in PBS and recovered by centrifugation. They were mixed with IntestiCult/

Matrigel mix (1 : 1 volume), plated in 50 μ L drops, and covered with 900 μ L of culture medium in 12-well plates. Twenty-four hours after replication, organoids were treated with 4-OH-tamoxifen (0.2 mg·mL⁻¹; Sigma-Aldrich H6278) or DMSO (control) for 24 h and monitored for several days after treatment. The cultures were recovered on day 5 for genomic DNA (gDNA) and RNA extraction. Pictures were taken over the days of culture using a Zeiss AxioVert (Marly le roi, France) inverted microscope with a 10 \times objective.

2.9. Genomic DNA extraction and PCR analysis

We extracted gDNA from Apc^{+/^{fl}/Villin-Cre^{ERT2} and Apc^{+/^{fl} enteroids at D5 using the Nucleospin Genomic DNA from Tissue kit (Machery-Nagel). The presence of the *Apc*-mutated allele was detected by PCR using specific primers listed in Table S1.}}

2.10. RNA extraction and RTqPCR

We extracted total RNA using the Nucleospin RNA Kit (Machery-Nagel, Hoerd, France). We performed DNase digestion on all samples to remove contaminating gDNA and reverse transcription (RT) of total RNA with iScript reverse transcriptase (Bio-Rad), according to the manufacturer's instructions. We conducted PCR on all preparations to amplify a housekeeping gene (*Hprt/HPRT*) for which the primers are located on different exons of the corresponding gene to further exclude gDNA contamination after RT. For qPCR approaches, we used SYBR qPCR Premix Ex Taq II (Tli RNaseH Plus; Takara) in a CFX Connect apparatus (Bio-Rad). In each sample, specific mRNA expression was quantitated using the $\Delta\Delta C_t$ method, and values were normalized against *Ppib/PPIB* levels. The primers used are listed in Table S1.

2.11. Statistical analysis

Statistical analyses were conducted using GRAPHPAD PRISM software (version 8; GraphPad Software Inc., San Diego, CA, USA), and the level of significance was established as *P*-value < 0.05.

3. Results

3.1. Expression of *THRA* in human colorectal cancer

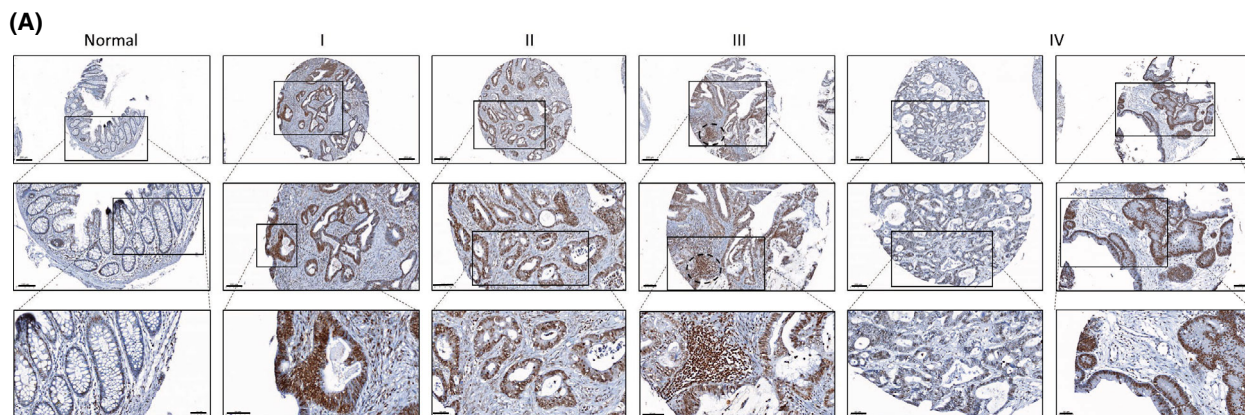
Our previous studies showed increased expression of the TR α 1 protein in CRC from patients compared with

the normal colon [15]. Here, we enlarged this study and used an approach of IHC on a tissue microarray (TMA) to analyze TR α 1 expression in a CRC cohort of patients with different tumor stages (Fig. 1, Fig. S2; Table S3 summarizes all known characteristics of the samples). TR α 1 labeling intensity was scored in each sample, including the tumor and normal tissue as well as the stromal cells and the immune infiltrate (Fig. 1B, Table S3). Compared with the normal colon, TR α 1 immunolabeling was clearly stronger in almost all tumors and at all tumor stages. Even if a clear difference was not observed based on the tumor stage, we noticed that stage II and stage III tumor samples frequently presented TR α 1-positive immune infiltrating cells (Fig. 1, Table S3), as determined by morphological characteristics [48,49]. It is worth emphasizing, however, that evident intratumor heterogeneity was observed, with some cells or tumoral parts strongly labeled and some cells or tumoral zones more lightly labeled or negative. In addition, high-magnification images enabled us to distinguish stromal cells expressing different levels of TR α 1 and TR α 1-negative cells. In stage IV CRC, we could identify tumors displaying variable levels of TR α 1 (i.e., in comparing the two images of stage IV), clearly indicating intertumor heterogeneity of TR α 1 expression. *THRA* gene expression was also determined in the human TCGA COAD cohort (Fig. S3). Despite the absence of a difference when globally comparing CRCs and normal tissues likely due to the high heterogeneity (Fig. S3A), we confirmed increased *THRA* expression in the CMS2 high-Wnt molecular subtype [23] (Fig. S3B), as previously described in another cohort [15].

Altogether, these results reinforce our previous data showing that TR α 1 is upregulated in human CRC and is correlated with Wnt pathway activity.

3.2. *THRA* promoter analysis

Because of the upregulation of *THRA* in the CRC cohorts and the specific expression of TR α 1 in intestinal crypt cells [14], we wanted to determine the molecular basis of its expression regulation. *In silico* analysis of 3238 bp of the *THRA* promoter region showed the presence of several putative binding sites for transcription factors, such as TCF7L2, RBPJ, and CDX2, that are fundamental to intestinal physiology and are altered in CRC [50] (Fig. 2). Of note, other studies have also shown β -catenin-binding sites in the boundaries of the *THRA* gene [51]. The *THRA* promoter region was cloned into a luciferase reporter vector (*THRA*-luc, Fig. S1A), and its activity was analyzed in transient transfection experiments. We implemented



(B)

TRα1 IHC Sample, Map	Tumor	Normal	Stroma	Immune Infiltration
Normal colon, I3	NP	+/-	+/-	NI
Stage I, E5	++	NP	++	NI
Stage II, B2	++	NP	++	NI
Stage III, G2	++	NP	+	++
Stage IV, A4	+	NP	+	NI
Stage IV, D2	++	NP	++	NI

NI: not identified
NP: not present

Fig. 1. Expression of TRα1 in human TMA of colorectal samples. (A) Immunohistochemical analysis of TRα1 expression in a CRC cohort of patients with different indicated tumor stages (I, II, III, and IV) and in the normal colon. Scale bar: 200 μm (low magnification), 100 μm (medium magnification), 50 μm (high magnification). (B) Scoring of TRα1 protein levels: -, negative; +/-, low; +, positive; ++, highly positive. The scoring was performed independently by two individuals.

two steps to take into account the genetic heterogeneity of CRC and avoid bias in the experiments. First, we performed the study using three different human COAD cell lines—Caco2, SW480, and HCT116—displaying different mutations of genes or pathways that are more frequently altered in CRC [52–55] (Fig. S4A). Second, all cell lines were maintained in culture medium supplemented with the same concentration of serum, ensuring comparable amounts of growth factors that could potentially influence subsequent analyses [56]. We also verified TRα1 expression by RTqPCR and noticed that SW480 cells presented significantly higher mRNA levels than Caco2 and HCT116 cells.

When we started the promoter analysis, we observed *THRA*-dependent luciferase basal activity in every cell line, compared with the pGL3-basic vector (Fig. S5A). In addition, upon cotransfection with the Wnt transcriptional regulators β-catenin/TCF1, regardless of the mutational background of the cells, the activity of

the *THRA* promoter was significantly increased (Fig. 3A–C, left panels). The results on the Notch pathway relative to the *THRA* promoter were more complex, as cotransfection of the Notch intracellular domain (NICD) decreased the luciferase activity in Caco2 and HCT116 cells but had no effect on SW480 cells (Fig. 3A–C, middle panels). When we analyzed the effect of CDX2 on *THRA*, we observed positive regulation of luciferase activity in all cell lines (Fig. 3A–C, right panels). The TopFlash, *RBPJ*-luc, and *hLI*-luc vectors were used, respectively, as the positive controls for Wnt, Notch, and CDX2 activities. Finally, no effect of the transcription factors could be detected when using the pGL3-basic vector (Fig. S5B).

Taken together, these data show that *THRA* promoter activity is positively regulated by the Wnt/β-catenin pathway and CDX2 in human colorectal adenocarcinoma cell lines. The Notch pathway plays a more complex role and behaves as a negative regulator or has no effect on *THRA* promoter.

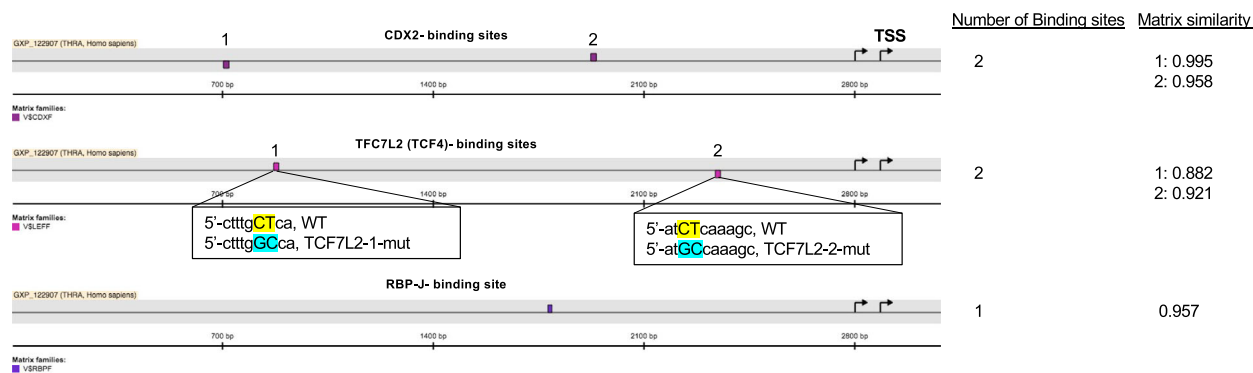


Fig. 2. *THRA* promoter *in silico* analysis. *In silico* analysis of 3238 bp of the *THRA* promoter revealed the presence of binding sites for different transcription factors, such as CDX2, TCF7L2, and RBPJ. The insets below the TCF7L2-binding sites show the changes introduced in the mutant promoters compared to the WT. The approximate location of the binding sites in the scheme is assigned from the 5' portion of the promoter. On the right, the number of putative binding sites and the matrix similarity for each site compared with the canonical binding site are indicated (1 = 100% similarity).

3.3. Analysis of *THRA* promoter upon modulation of CDX2 expression and signaling pathway activity

To further link *THRA* promoter activity with Wnt, Notch, and CDX2, we used approaches involving modulation by siRNA (CDX2) or small molecules (Wnt and Notch). In the case of CDX2, we confirmed its stimulatory effect on *THRA* activity, which was lost in CDX2-KD cells transfected with siRNA@CDX2 (Fig. 4). However, siRNA@CDX2 *per se* did not decrease *THRA* activity (Fig. 4). Treatment of the cell lines with Notch agonists or antagonists confirmed the complex scenario observed in the cotransfection experiments described in the previous paragraph (not shown). We then decided to focus specifically on more in-depth analysis of the Wnt pathway, considering the cross-talk and synergy between TR α 1 and Wnt reported in previous studies [14,15,57].

The three cell lines were treated with the Wnt activator CHIR99021 (CHIR) [41] or the Wnt antagonist IWP4 for 24 h [42]. As expected, CHIR increased the activity of both *THRA*-luc and TopFlash (Fig. 5A). IWP4 induced a significant decrease in TopFlash activity in all cell lines compared with the control (Fig. 5B). However, when we analyzed the action of this molecule, it clearly inhibited *THRA*-luc activity only in HCT116 cells (Fig. 5B). We also evaluated the effect of the Wnt modulators on endogenous TR α 1 expression and compared it with the cotransfection of β -catenin and TCF1 (Figs S6 and S7). Although we confirmed a difference in the response to Wnt modulators depending on the cell line (Fig. S6), the cotransfection of cells with β -catenin/TCF1 resulted in increased TR α 1 mRNA and protein expression in all cell lines (Fig. S7A,B).

Overall, we confirmed that high CDX2 levels regulated the *THRA* promoter and that its activity was increased by the Wnt agonist CHIR. In addition, Wnt stimulation also affected endogenous TR α 1 expression.

3.4. Mutational and functional analyses of the *THRA* promoter

To definitively link the *THRA* promoter activity with the Wnt/ β -catenin signaling pathway, we performed experiments on the *THRA*-luc construct carrying a mutation in each of the TCF7L2 sites (*THRA*-mut1-luc and *THRA*-mut2-luc vectors) or in both TCF7L2 sites (*THRA*-dmut-luc vector) (Fig. S1B–D). We performed experiments in parallel with *THRA*-luc and the mutated versions in the three cell lines used in the previous experimental protocols in the presence or absence of cotransfected β -catenin/TCF1 (Fig. 6A). In both *THRA*-mut1-luc and *THRA*-mut2-luc, the induction of *THRA*-dependent luciferase activity by β -catenin/TCF1 significantly decreased in the three cell lines compared to that observed with the WT promoter (Fig. 6A). This effect was even more evident when using the double mutant vector, as the induction of *THRA*-dependent luciferase activity by β -catenin/TCF1 was strongly affected in all cell lines. Importantly, the mutations in each or both TCF7L2 sites decreased the *THRA*-dependent luciferase basal activity in all cell lines compared with the nonmutated promoter.

To further confirm the importance of Wnt activity on the *THRA* promoter, we also performed experiments using a vector expressing a mutated form of TCF1 that acts as a dominant-negative (TCF1-DN) vis-à-vis the WT protein [58]. By cotransfecting the

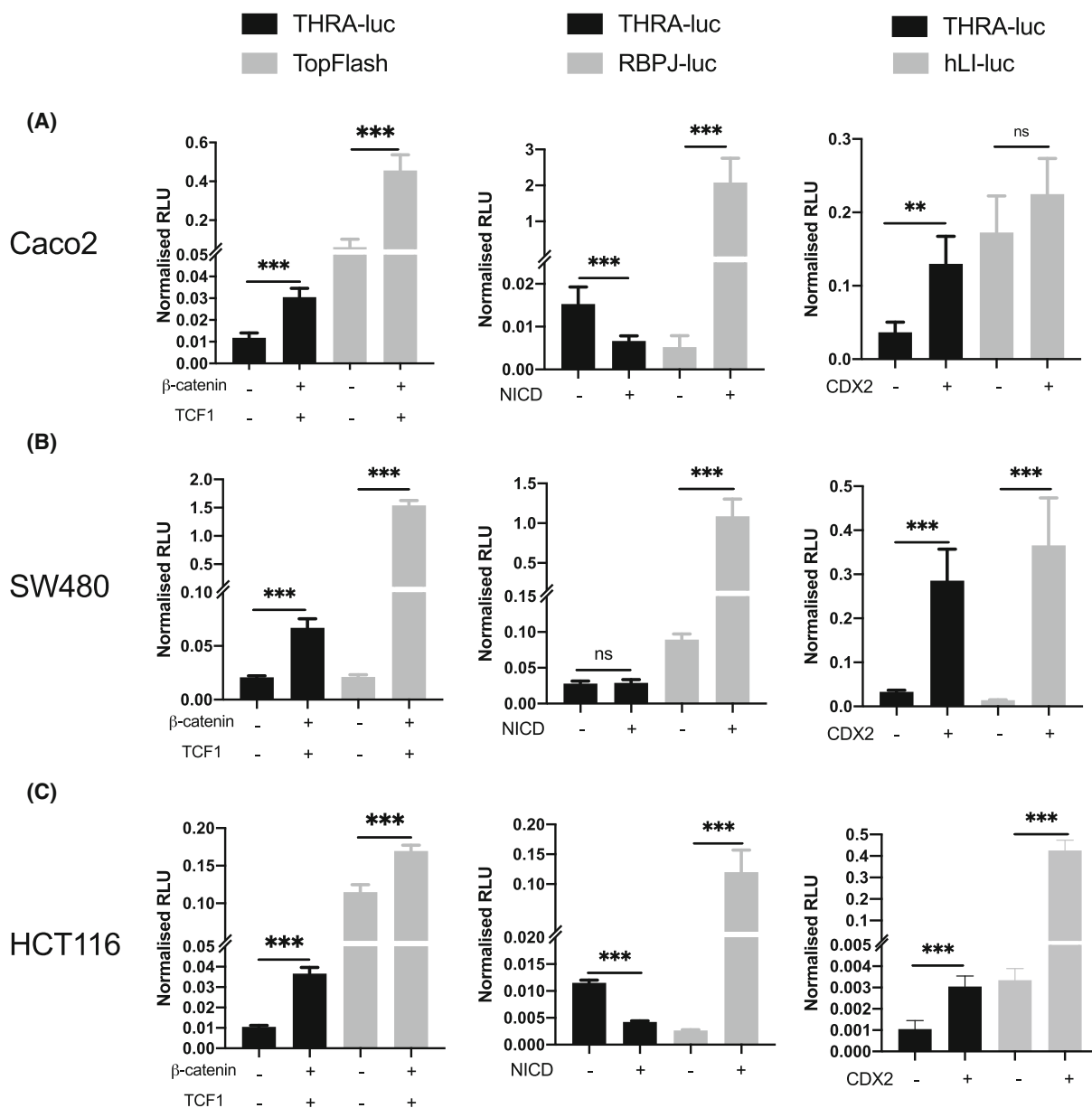


Fig. 3. Modulation of *THRA* promoter activity in human adenocarcinoma cell lines by Wnt, notch, and CDX2. (A–C) Caco2 (A), SW480 (B), and HCT116 (C) cells were transfected with the *THRA*-luc vector alone or cotransfected with different transcription factors. The left panels show results obtained with the Wnt cofactors β-catenin/TCF1; the central panels show results obtained with the notch pathway activator NICD; and the right panels show results obtained with CDX2. TopFlash, *RBPJ*-luc, and *hLI*-luc were used as positive controls for Wnt, notch, and CDX2, respectively. Graphs show the mean ± SD (*n* = 6) of normalized relative luciferase units (RLU) from at least two independent experiments, each conducted in six replicates. ns, nonsignificant, ***P* < 0.01, and ****P* < 0.001 by unpaired, two-tailed Student’s *t*-test.

TCF1-DN vector, we observed a significant decrease in *THRA*-luc activity in Caco2 and HCT116 cells but only a slight decrease in *THRA*-luc activity in SW480 cells (Fig. 6B). When we re-expressed increasing amounts of β-catenin (from 50 ng to 500 ng) under suppressed Wnt conditions, we observed an increased

THRA-luc activity that differed among the cell lines. In Caco2 cells, a dose–response effect to increased β-catenin amounts was observed. In SW480 and HCT116 cells, the luciferase activity increased significantly compared with the TCF1-DN condition but rapidly reached a plateau and could not be stimulated

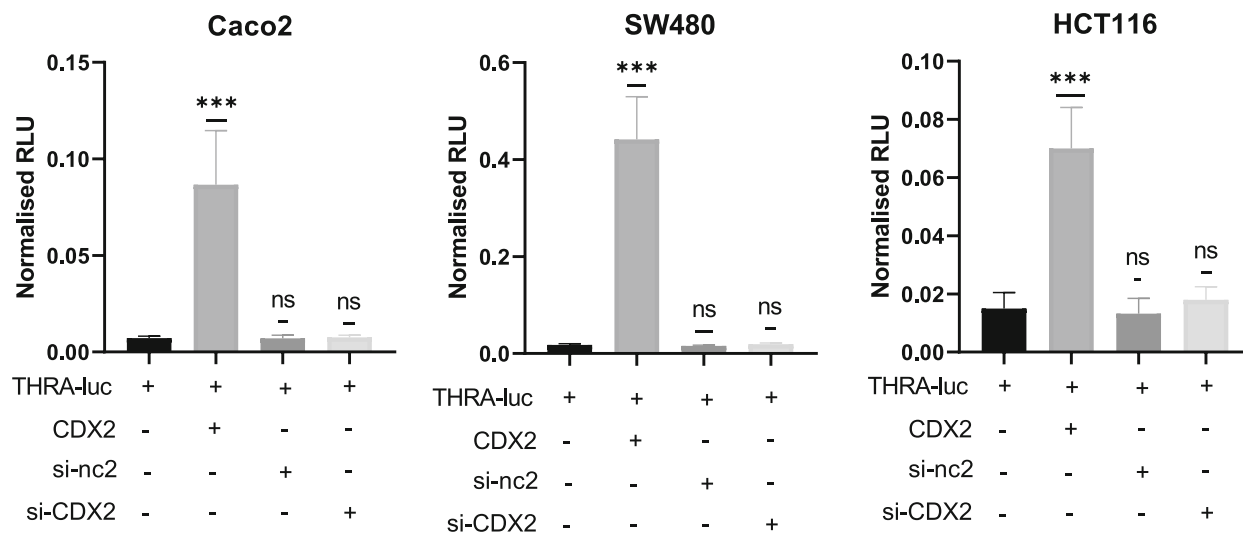


Fig. 4. Effect of CDX2-KD on *THRA*-luc activity. Analysis of the effect of silencing CDX2 on the *THRA* promoter activity in the adenocarcinoma cell lines Caco2, SW480, and HCT116, as indicated. Graphs show the mean \pm SD ($n = 6$) of normalized relative luciferase units (RLU) from at least two independent experiments, each conducted in six replicates. ns, nonsignificant and *** $P < 0.001$ by unpaired, two-tailed Student's *t*-test.

by higher β -catenin concentrations (Fig. 6B). The efficacy of TCF1-DN was validated using the TopFlash control vector (Fig. S8).

The above results and those described in the previous paragraphs prompted us to determine whether the regulation of the *THRA* promoter by the Wnt effectors β -catenin/TCF was mediated by direct binding to chromatin. For this aim, we used a ChIP approach in the three cell lines. ChIP was performed by using anti- β -catenin or IgG (negative control). As shown in Fig. 7, β -catenin bound to the *THRA* promoter regions containing the TCF7L2 sites. The specificity of β -catenin binding was validated on *AXIN2*- and *MYC*-positive control promoters (Fig. S9), whereas no specific binding was detected on the *HPRT* or *PPIB* genes (Fig. S9).

These results underline the control of the *THRA* promoter by the Wnt/ β -catenin pathway in human COAD cell lines, which is exerted through the functional TCF7L2-binding sites located 3 kb upstream of the transcription start site. In addition, promoter control is achieved by direct binding of β -catenin to chromatin.

3.5. Stimulation of TR α 1 expression by activated Wnt in mouse enteroids

The previous results compelled us to investigate the effect of activating Wnt on TR α 1 expression in a more complex and physiological model, which eventually recapitulated the steps of Wnt activation in early

intestinal lesions. For this purpose, we used *Apc*^{+/^{fl}/*Villin-Cre*^{ERT2} and *Apc*^{+/^{fl} mice to generate organoids from the small intestine. In *Apc*^{+/^{fl}/*Villin-Cre*^{ERT2} enteroids, mutation of the *Apc* gene was induced by the addition of 4-OH-tamoxifen to the culture medium, resulting in the increase in Wnt activity [46]. *Apc*^{+/^{fl} enteroids have been used as negative controls for tamoxifen treatment, given that they do not express the *Cre*^{ERT2} protein.}}}}

Enteroids of different genotypes were freshly prepared and cultured for 7 days before replication. One day after replication, they were treated with tamoxifen or DMSO (control) for 24 h (Fig. 8A). The induction of the mutated *Apc* allele by tamoxifen in *Apc*^{+/^{fl}/*Villin-Cre*^{ERT2} enteroids was validated by PCR on genomic DNA, while no effect of tamoxifen was observed in *Apc*^{+/^{fl} enteroids (Fig. 8B). The cultures were monitored under a microscope to follow their growth depending on the genotype and conditions for 4 days after treatment (Fig. 8C). In control condition, independent of the genotype, enteroids underwent typical development during the days in culture, characterized by the outgrowth and lengthening of buds (Fig. 8C). Consistent with previous reports [59,60] upon tamoxifen treatment of *Apc*^{+/^{fl}/*Villin-Cre*^{ERT2} enteroids, we observed a change in their morphology, with a reduced length of buds and enlargement of the central body because of the lack of the Wnt gradient [61] (Fig. 8C, upper panel). On the contrary, tamoxifen treatment of *Apc*^{+/^{fl}-derived enteroids produced no obvious changes in their morphology (Fig. 8C,}}}}

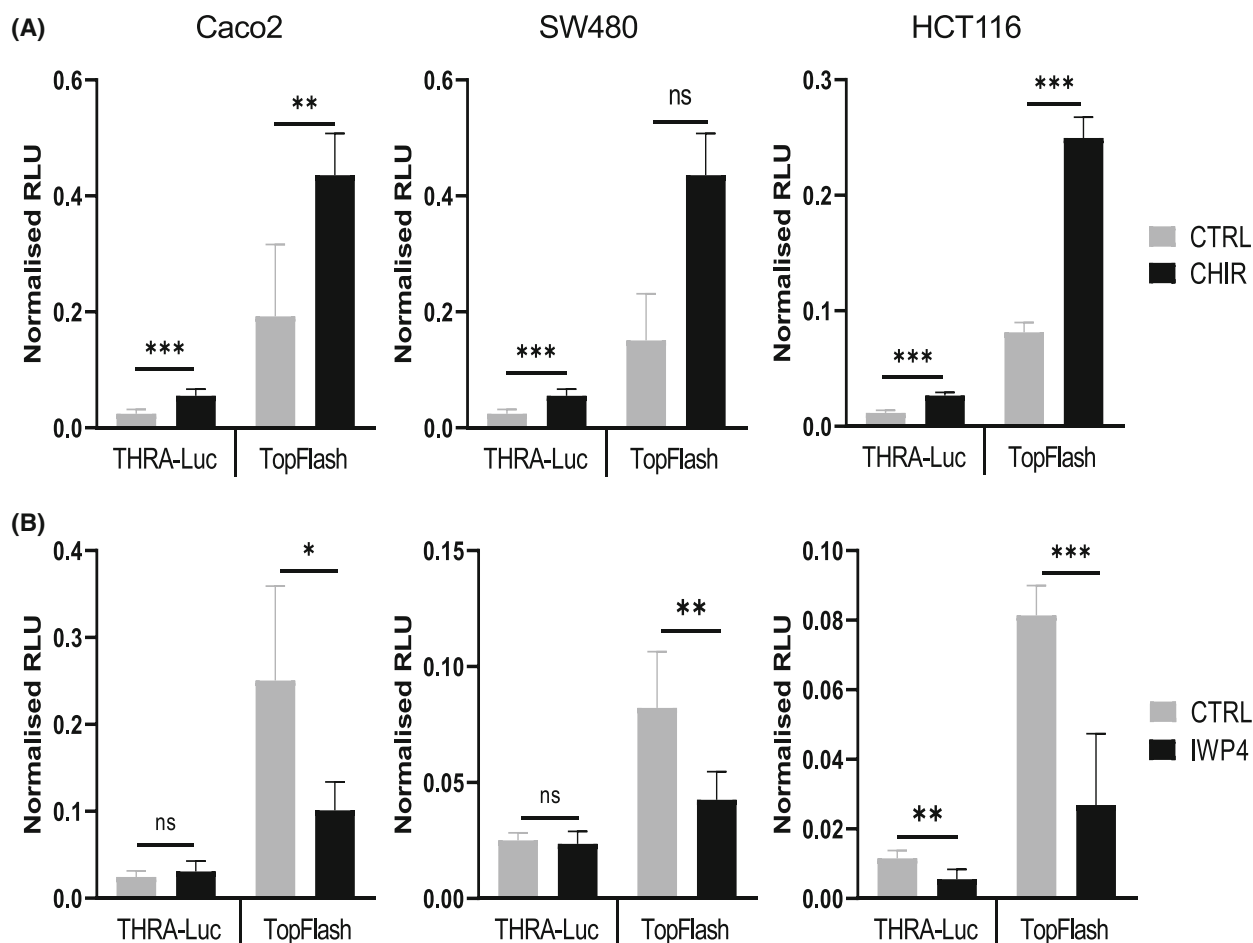


Fig. 5. Modulation of *THRA*-luc activity by the Wnt agonist and antagonist. Analysis of *THRA*-luc and TopFlash activity in the presence of the Wnt agonist CHIR99021 (A) and the Wnt antagonist IWP4 (B) in Caco2, SW480, and HCT116 cells, as indicated. Graphs show the mean \pm SD ($n = 6$) of normalized relative luciferase units (RLU) from at least two independent experiments, each conducted in six replicates. ns, nonsignificant, $*P < 0.05$, $**P < 0.01$, and $***P < 0.001$ by unpaired, two-tailed Student's *t*-test.

lower panel). We analyzed in these enteroids the expression of *TRα1* and *Wif1*, a negatively regulated direct *TRα1* target gene [15], together with a panel of Wnt-responsive genes. As expected, upon tamoxifen treatment, *Apc*^{+/*fl*}/*Villin-Cre*^{ERT2} enteroids displayed increased mRNA levels of the Wnt targets *Ccnd1*, *cMyc*, *Axin2*, and *Cd44* (Fig. 8D). Importantly, in accordance with the data on the promoter analyses, *TRα1* was significantly stimulated in these mutated-*Apc* enteroids, and *Wif1* was downregulated (Fig. 8D). RTqPCR analysis on *Apc*^{+/*fl*} enteroids showed no effect of tamoxifen treatment (Fig. S10).

4. Discussion

It has been more than 50 years since the *THRA* gene was cloned and characterized as a homolog of the *v-erbA* gene, which is involved in neoplastic

transformations leading to acute erythroleukemia and sarcomas [24,25], strongly suggesting its link with oncogenesis. Because of this peculiarity, it was quite logical to assume that *TRα1*, which is produced by this locus, behaves as an oncogene. It has also been speculated that a mutated *TRα1* instead of the WT form can have a pro-tumoral function. Indeed, some data have described mutations in the *THRA* gene in gastric cancers (essentially deletions) [62], and mouse models have assigned oncogenic functions to mutated *TRα1* [63,64]. Recent studies by our laboratory, however, clearly indicated the protumoral function of WT *TRα1* when overexpressed in the mouse intestine and colon [14]. Studies in human CRC cohorts also allowed us to establish the relevance of observations from mice to human pathology [15]. In this context, the cross-regulations between *TRα1* and the Wnt/ β -catenin pathway are multiple, and in the case of tumor formation and progression, they

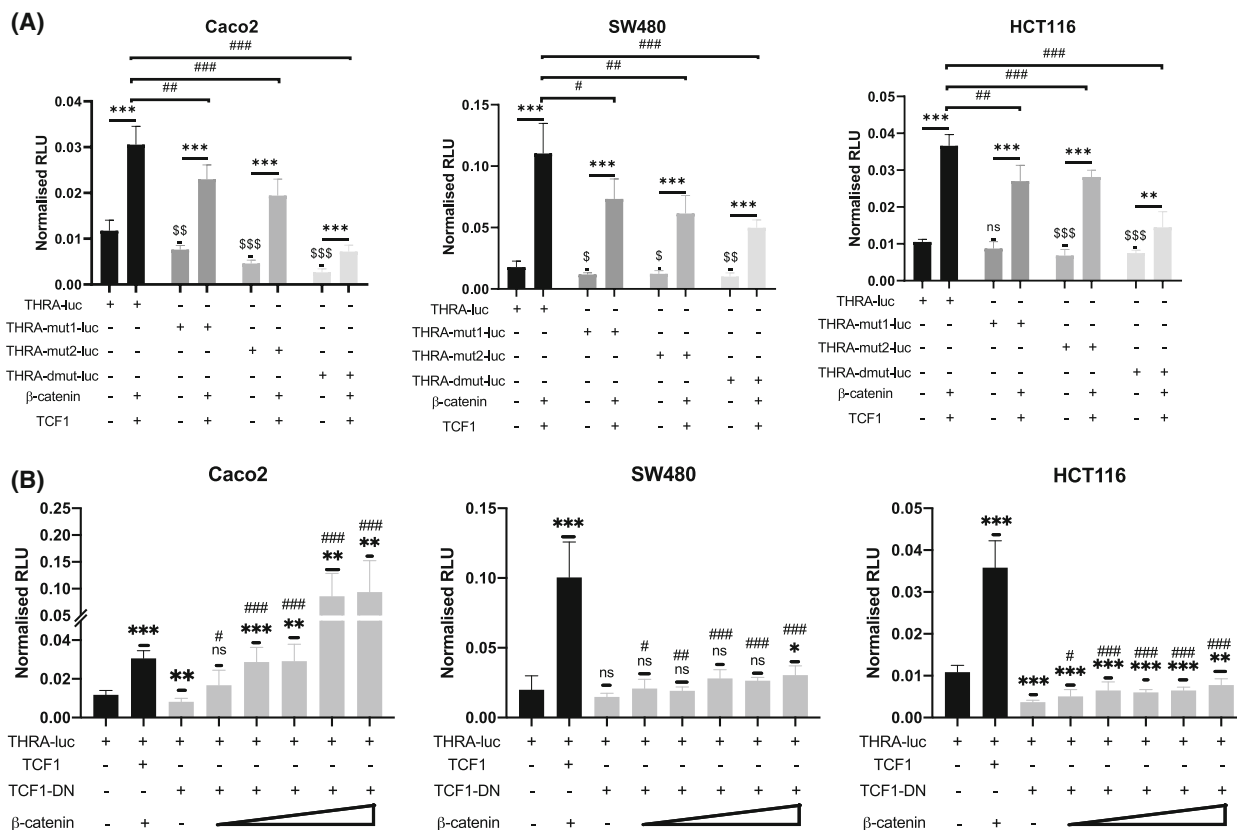


Fig. 6. Mutations and Wnt-blocking analyses on *THRA* promoter activity. (A) TCF7L2-binding site mutations. *THRA*-luc or the different *THRA*-Mut-luc constructs, as indicated, were transfected alone or cotransfected with β-catenin and TCF1. Experiments were performed in Caco2 (left panel), SW480 (central panel), and HCT116 (right panel) cells. The graphs show the mean ± SD ($n = 6$) of the normalized relative luciferase units (RLUs) from at least two independent experiments, each of which were conducted with six replicates. ns, nonsignificant, $**P < 0.01$, and $***P < 0.001$ comparing the basal activity with the activity after cotransfection. # $P < 0.05$, ## $P < 0.01$ and ### $P < 0.001$ comparing *THRA*-luc with the different mutated constructs after cotransfection with β-catenin/TCF1. \$ $P < 0.05$, \$\$ $P < 0.01$ and \$\$\$ $P < 0.001$ comparing the basal activity of *THRA*-luc with that of the different mutated constructs. Statistics were performed using unpaired, two-tailed Student's *t*-test. (B) The *THRA*-luc construct was transfected alone or cotransfected with TCF1-DN and different amounts of β-catenin (0, 50, 100, 200, 300, and 500 ng), as indicated. Experiments were performed in Caco2 (left panel), SW480 (central panel), and HCT116 (right panel) cells. The graphs show the mean ± SD ($n = 6$) of the normalized relative luciferase units (RLUs) from at least two independent experiments, each of which were conducted with six replicates. ns, nonsignificant, $*P < 0.05$, $**P < 0.01$, and $***P < 0.001$ compared with the basal promoter activity. ns, nonsignificant, # $P < 0.05$, ## $P < 0.01$, and ### $P < 0.001$ by comparing the activity of *THRA*-luc cotransfected with TCF1-DN alone with the activity in the presence of different concentrations of β-catenin. Statistical analysis was performed based on an unpaired, two-tailed Student's *t*-test.

depend on mutations in the tumor suppressor gene *Apc/APC* [14,15]. Indeed, the *THRA* gene is frequently over-expressed in CRC molecular subtypes, particularly in CMS2 characterized by high Wnt [15]. We would like to emphasize that our previous study also showed its significant association with CMS3, which is characterized by high metabolic status. Differences among the cohorts, in microarray versus RNA-seq analyses and among the normal counterparts analyzed may account for the discrepancy. Higher TRα1 expression was, however, definitively clear when considering the IHC analysis in the TMA of CRCs, where we observed a strong

increase in TRα1 expression in tumors at all stages compared with the normal colon. The results also point to great heterogeneity in tumor parts and/or stromal cells strongly or poorly expressing TRα1. In addition to being upregulated in CRCs, in the normal intestine, TRα1 shows a distinct expression pattern that follows the gradient of Wnt and Notch activities [6,14]. However, what determines this specific expression domain was unknown and it was also unknown what are the effectors of its increase in CRCs. Of note, only a few studies have analyzed the molecular basis of *THRA* gene regulation [26–29], and none were performed in the

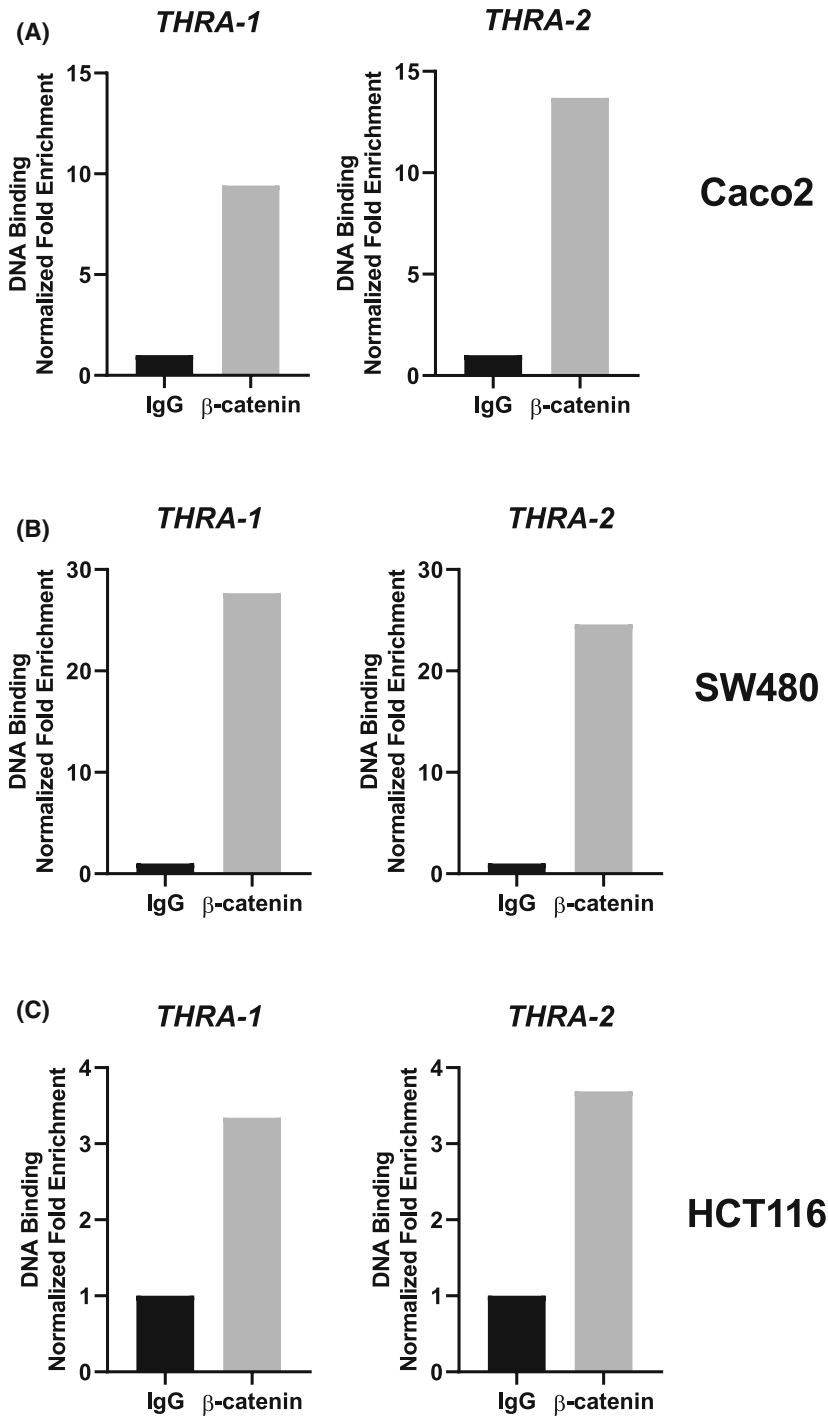


Fig. 7. Chromatin occupancy of β -catenin in the *THRA* gene promoter. CHIP analysis was performed with chromatin prepared from (A) Caco2, (B) SW480, and (C) HCT116 cells and immunoprecipitated using an anti- β -catenin or IgG (negative control). qPCR was performed using specific primers covering each TCF7L2-binding site within 3 kb of the *THRA* promoter. The results are representative of two independent experiments. Histograms represent the fold enrichment of specific β -catenin/DNA binding normalized to the input and compared with the IgG condition (= 1).

context of cancer. This is the first study analyzing the mechanisms of *THRA* expression regulation in CRCs.

We performed *in silico* analysis on the 3 kb of *THRA* promoter and showed potential binding sites for transcription factors involved in intestinal homeostasis that impact SC biology and CRC development. CDX2 encodes a protein that is a master regulator of

intestinal epithelial cell identity [32,65], and is involved in SC biology [66,67]. Both tumor inducer and tumor suppressor roles have been indicated for CDX2 [23,68–71] and its downregulation is often associated with CRCs [23,35,68,69,72,73]. However, in some cases CDX2 has been reported to be overexpressed in CRCs, and in these cases its overexpression stimulates

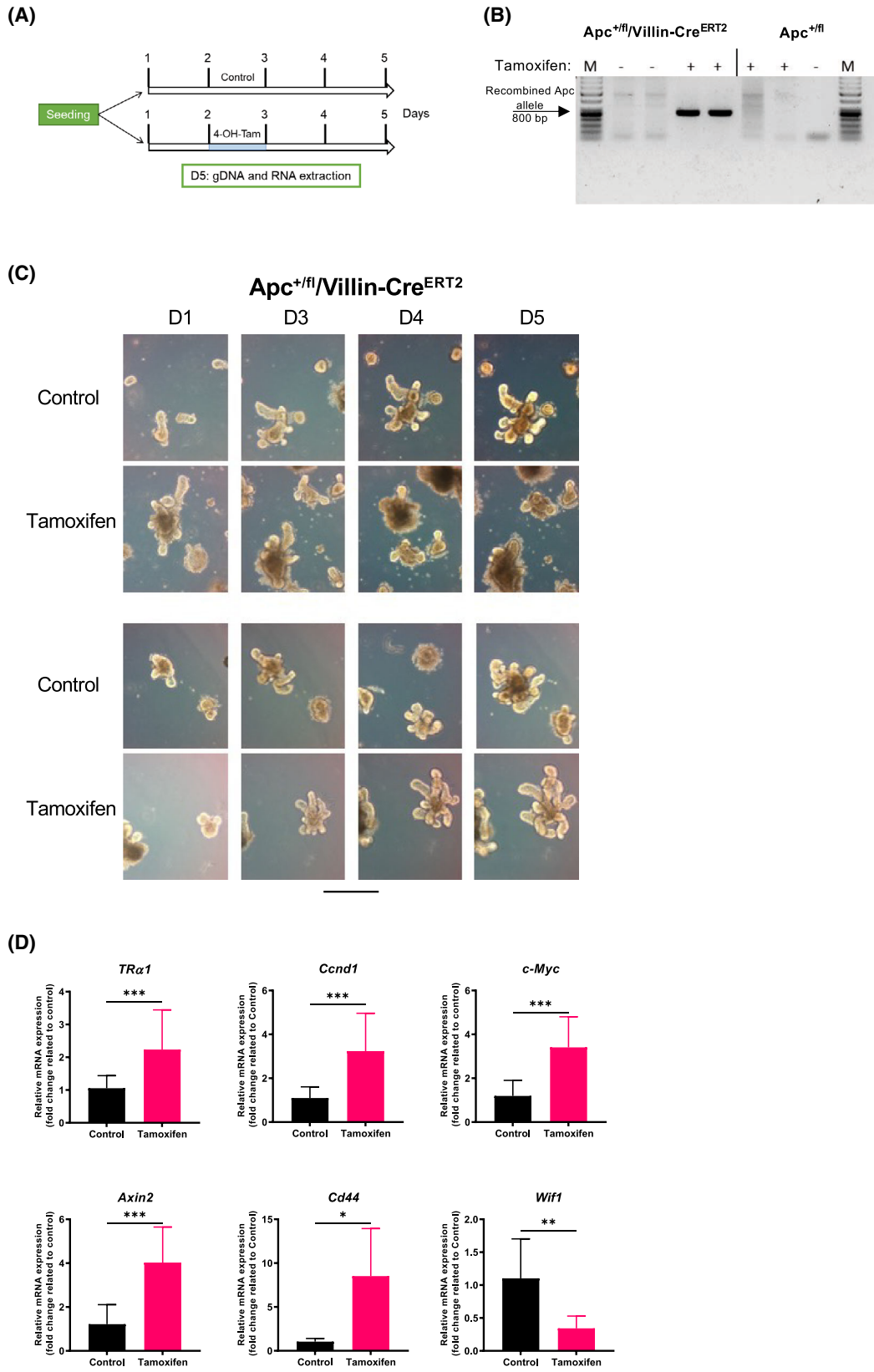


Fig. 8. TR α 1 modulation by the induction of the *Apc* mutation in mouse enteroids. (A) Schematic diagram of the protocol used for *ex vivo* enteroid cultures. (B) PCR analysis on gDNA extracted from enteroids of different genotypes and treatments, as indicated, to verify the recombination of the *Apc* gene after tamoxifen treatment. Specific primers recognizing the mutated allele were used. Note that the band corresponding to mutated *Apc* was detected only in *Apc*^{+fl}/*villin-Cre*^{ERT2} tamoxifen-treated organoids. (C) Bright-field pictures of enteroids obtained from *Apc*^{+fl}/*villin-Cre*^{ERT2} and *Apc*^{+fl} mice treated with tamoxifen or not treated (control). Pictures were taken at different days of culture, as indicated, using a Zeiss AxioVert inverted microscope with a 10 \times objective. Scale bar = 10 μ m. (D) RT-qPCR analysis of the indicated genes performed on RNA isolated from *Apc*^{+fl}/*villin-Cre*^{ERT2} enteroids treated with tamoxifen or not treated (control), as indicated. Histograms represent the mean \pm SD ($n = 6$), and data are expressed as the fold change relative to the control condition (= 1). *Ppib* was used as a reference gene. * $P < 0.05$, ** $P < 0.01$ and *** $P < 0.001$ by unpaired, two-tailed Student's *t*-test. The results in B–D are representative of three independent experiments, each conducted in six replicates.

tumorigenesis, suggesting an oncogenic function [74]. We observed here that high CDX2 levels strongly upregulated the *THRA* promoter in all adenocarcinoma cell lines analyzed despite their different genetics and mutation statuses. *Cdx2*-KO mice display a decreased expression of the *Thra* gene [69], further strengthening our results on the positive control of *THRA* by CDX2. Interestingly, our previous studies showed that *Thra*-KO mice presented increased *Cdx2* mRNA expression and that *CDX2* promoter activity was blunted by TR α 1 in transfection experiments [75,76]. Finally, our unpublished observations point to a more complex interplay between *TR α 1* and *CDX2* in CRC cohorts, as we observed tumors with opposite expression levels of *TR α 1* and *CDX2*, as well as tumors displaying a direct correlation between them (both upregulated or downregulated) (M. Plateroti & J.-N. Freund, personal communication). Future studies will surely shed light on the molecular and cellular mechanisms responsible for this complex interrelation.

The Notch pathway showed intriguing action on the *THRA* promoter, which appears to be dependent upon the cellular context. We observed that NICD transfection decreased *THRA* activity in Caco2 and HCT116 cell lines but had a stimulatory function in SW480 cells. Additionally, the use of small molecules, suggested to behave as agonists or antagonists of Notch, was hampered by the difficulty of definitively assigning specific roles as activators or inhibitors to these molecules. According to the literature, it appears clear that each of their roles is much larger and goes beyond the control of the Notch pathway [72–75]. It is also worth noting that the Notch pathway has complex cross-talk with the Wnt pathway, possibly explaining the puzzling results that we observed [22,37,76–80]. Given the regulation of *THRA* gene expression by Wnt (also discussed in the next paragraph), we assume that the three cell lines analyzed, which present different levels of Wnt activity (Fig. S4), might respond differently to Notch, thus explaining the different effects observed on *THRA* activity.

Our previous work described complex cross-talk between TR α 1 and the Wnt pathway [6,7,10], but we did not analyze whether Wnt could affect *THRA/Thra* expression. Here, we show that in cell lines, activating Wnt in all cases and by all approaches resulted in increased *THRA* promoter activity. This regulation also applied to endogenous TR α 1 expression upon β -catenin/TCF cotransfection. The direct β -catenin binding of the promoter regions containing TCF7L2-binding sites strongly supports direct transcriptional regulation. The effect of the Wnt agonist CHIR and Wnt antagonist IWP4 on *THRA* activity and endogenous TR α 1 was more complex to analyze. The drugs were chosen based on the literature [41,42] and validated using the Wnt-reporter TopFlash in all cell lines. We hypothesize that the differences in responsiveness or lack of responsiveness may depend on the different genetic and epigenetic backgrounds of the cell lines, and these molecules, as previously noted for the Notch agonists and antagonists, could have various targets [77–79]. In relation to the genetic background with respect to the Wnt pathway, Caco2 cells have a loss-of-function (LOF) mutation of the *APC* gene and a silent mutation in the *CTNNB1* gene (coding β -catenin). SW480 cells have a LOF *APC* mutation and a WT *CTNNB1* gene. HCT116 cells have a gain-of-function *CTNNB1* mutation [54,81]. In addition, these cell lines have different mutations in additional pathways that can also impact Wnt [54,55], underscoring the complexity encountered when working with these model systems.

Importantly, however, in the physiological context of mouse enteroids, which recapitulate the complexity, organization and hierarchy of the intestinal epithelium [82], stimulating Wnt by *Apc* gene mutation increased TR α 1 expression. Altogether, considering our previous and new results, we propose the model illustrated in Fig. 9. High Wnt, as well as other transcription factors, maintains a basal level of TR α 1 expression in normal intestinal crypts, where TR α 1 integrates and interacts with other key pathways, such as Wnt and Notch, as well as CDX2 [30–32], to participate in

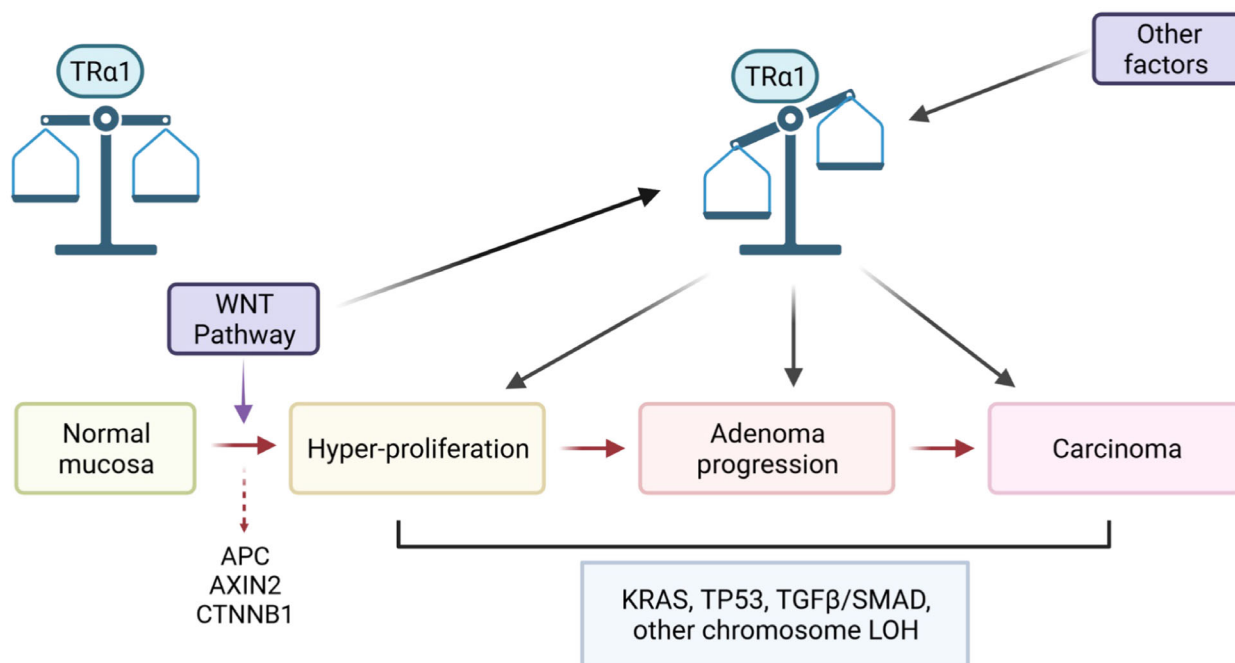


Fig. 9. Interplay between TR α 1 and the Wnt pathway and correlation with gene deregulation during intestinal tumorigenesis. The picture summarizes the known sequential genetic alterations that are frequently associated with colorectal tumorigenesis in humans. *APC/AXIN2/CTNNB1* gene mutations, which are responsible for Wnt/ β -catenin overactivation, are key events that occur during the early stage of cell transformation. The other indicated mutations are more frequently associated with later stages [88]. Interestingly, together with the control of the Wnt pathway by TR α 1 and its association with the various steps in CRC (hyperproliferation, adenoma progression, and carcinoma generation) [14,15], our new data point to regulation of the *THRA* promoter by the Wnt pathway and regulation of TR α 1 expression by increased Wnt activity in very early stages of tumor development. LOH, loss of heterozygosity. The figure was created with [BioRender.com](https://www.biorender.com) (agreement number: TX23QDYSJV).

intestinal homeostasis. Upon Wnt overactivation in the early stages of tumor development, TR α 1 expression increases, which in turn causes a further increase in Wnt activity responsible for crypt hyperplasia and hyperproliferation, as shown in *vil-TR α 1* mice [14]. Through its synergy with *Apc/APC*-dependent activated Wnt, TR α 1 accelerates tumor growth and participates in tumor progression, including cancer spreading [14] and possibly integrating other tumor processes not yet established. The increased aggressiveness of tumors displaying high TR α 1/high Wnt might depend on the strong decrease in the Wnt inhibitors *WIF1/Wif1*, *SOX17/Sox17*, and *FRZB/Frzb* that we have shown in mouse models and patient cohorts [15]. All of these proteins are silenced in CRC, and their silencing characterizes advanced stages and/or more aggressive tumors [83].

5. Conclusion

We showed here that several pathways and transcription factors control the expression of the *THRA* gene in the context of CRC. In particular, we unveiled the complex

action of the Wnt pathway on *THRA* promoter activity and TR α 1 expression. The significance and clinical relevance of high TR α 1 expression are of particular interest when considering CRC patients with altered TH levels [84,85] and/or undergoing chemotherapy treatments that potentially impact thyroid functionality [86,87].

Acknowledgements

We are grateful to Manon Pratiel, Pierre Lavogez, and Solene Faucheron for the assistance with animal handling and care within the animal facilities (CRCL and IRFAC). We thank Joel Uchuya-Castillo for realizing the very first steps of this work. We are indebted to Nicolas Gadot and the Research pathology platform (CRCL/CLB, Lyon) for the help in performing and analyzing the IHC on TMA. We also thank Isabelle Gross for helpful discussions and suggestions during the revision of the manuscript. The work was supported by the FRM (Equipes FRM 2018, DEQ20181039598), by the Inca (PLBIO19-289), and by the Ligue Contre le Cancer, Département Grand Est (01X.2020). MVG and TLR received support from

the FRM. DF and SB received support from the Inca. GDAG was supported by a fellowship from FAPESP (2017/19541-2).

Conflict of interest

The authors declare no conflict of interest.

Author contributions

MVG involved in conception and design, collection and assembly of data, data analyses and interpretation, and manuscript writing; TLR, DF, SB, GDAG, and PAFG involved in collection and assembly of data, data analyses, and interpretation; CD-D and J-NF involved in the development of tools, data analyses, and interpretation; MP involved in conception and design, assembly of data, data analyses, and interpretation, manuscript writing, and financial support. All authors approved the manuscript.

Data accessibility

The data that support the findings of this study are available from the corresponding author (plateroti@unistra.fr) upon request.

References

- Robinson-Rechavi M, Garcia HE, Laudet V. The nuclear receptor superfamily. *J Cell Sci.* 2003;**116**:585–6.
- Brent GA. Mechanisms of thyroid hormone action. *J Clin Invest.* 2012;**122**:3035–43.
- Cheng SY, Leonard JL, Davis PJ. Molecular aspects of thyroid hormone actions. *Endocr Rev.* 2010;**31**:139–70.
- Oetting A, Yen PM. New insights into thyroid hormone action. *Best Pract Res Clin Endocrinol Metab.* 2007;**21**:193–208.
- Mullur R, Liu YY, Brent GA. Thyroid hormone regulation of metabolism. *Physiol Rev.* 2014;**94**:355–82.
- Sirakov M, Kress E, Nadjar J, Plateroti M. Thyroid hormones and their nuclear receptors: new players in intestinal epithelium stem cell biology? *Cell Mol Life Sci.* 2014;**71**:2897–907.
- Frau C, Godart M, Plateroti M. Thyroid hormone regulation of intestinal epithelial stem cell biology. *Mol Cell Endocrinol.* 2017;**459**:90–7.
- Tanizaki Y, Bao L, Shi B, Shi YB. A role of endogenous histone acetyltransferase steroid hormone receptor coactivator 3 in thyroid hormone signaling during xenopus intestinal metamorphosis. *Thyroid.* 2021;**31**:692–702.
- Shi YB, Shibata Y, Tanizaki Y, Fu L. The development of adult intestinal stem cells: insights from studies on thyroid hormone-dependent anuran metamorphosis. *Vitam Horm.* 2021;**116**:269–93.
- Skah S, Uchuya-Castillo J, Sirakov M, Plateroti M. The thyroid hormone nuclear receptors and the Wnt/ β -catenin pathway: an intriguing liaison. *Dev Biol.* 2017;**422**:71–82.
- Modica S, Gofflot F, Murzilli S, D’Orazio A, Salvatore L, Pellegrini F, et al. The intestinal nuclear receptor signature with epithelial localization patterns and expression modulation in tumors. *Gastroenterology.* 2010;**138**:636–48.e12.
- Catalano V, Dentice M, Ambrosio R, Luongo C, Carollo R, Benfante A, et al. Activated thyroid hormone promotes differentiation and chemotherapeutic sensitization of colorectal cancer stem cells by regulating Wnt and BMP4 signaling. *Cancer Res.* 2016;**76**:137–1244.
- Godart M, Frau C, Farhat D, Giolito MV, Jamard C, Le Nevé C, et al. Murine intestinal stem cells are highly sensitive to modulation of the T3/TR α 1-dependent pathway. *Development.* 2021;**148**:dev194357.
- Kress E, Skah S, Sirakov M, Nadjar J, Gadot N, Scoazec JY, et al. Cooperation between the thyroid hormone receptor TR α 1 and the WNT pathway in the induction of intestinal tumorigenesis. *Gastroenterology.* 2010;**138**:1863–74.e1.
- Uchuya-Castillo J, Aznar N, Frau C, Martinez P, Le Nevé C, Marisa L, et al. Increased expression of the thyroid hormone nuclear receptor TR α 1 characterizes intestinal tumors with high Wnt activity. *Oncotarget.* 2018;**9**:30979–96.
- Sung H, Ferlay J, Siegel RL, Laversanne M, Soerjomataram I, Jemal A, et al. Global Cancer Statistics 2020: GLOBOCAN estimates of incidence and mortality worldwide for 36 cancers in 185 countries. *CA Cancer J Clin.* 2021;**71**(3):209–49.
- Fearon ER, Vogelstein B. A genetic model for colorectal tumorigenesis. *Cell.* 1990;**61**:759–67.
- Clapper ML, Chang WCL, Cooper HS. Dysplastic aberrant crypt foci: biomarkers of early colorectal neoplasia and response to preventive intervention. *Cancer Prev Res (Phila).* 2020;**13**:229–39.
- Aceto GM, Catalano T, Curia MC, Tong Q. Molecular aspects of colorectal adenomas: the interplay among microenvironment, oxidative stress, and predisposition. *Biomed Res Int.* 2020;**2020**:1–19.
- Suzui M, Morioka T, Yoshimi N. Colon preneoplastic lesions in animal models. *J Toxicol Pathol.* 2013;**26**:335–41.
- Barker N, Ridgway RA, van Es JH, van de Wetering M, Begthel H, van den Born M, et al. Crypt stem cells as the cells-of-origin of intestinal cancer. *Nature.* 2009;**457**:608–11.
- Fre S, Pallavi SK, Huyghe M, Laé M, Janssen KP, Robine S, et al. Notch and Wnt signals cooperatively

- control cell proliferation and tumorigenesis in the intestine. *Proc Natl Acad Sci USA*. 2009;**106**:6309–14.
- 23 Guinney J, Dienstmann R, Wang X, De Reyniès A, Schlicker A, Sonesson C, et al. The consensus molecular subtypes of colorectal cancer. *Nat Med*. 2015;**21**:1350–6.
 - 24 Thormeyer D, Baniahmad A. The v-erbA oncogene (review). *Int J Mol Med*. 1999;**4**:351–8.
 - 25 Sap J, Muñoz A, Damm K, Goldberg Y, Ghysdael J, Leutz A, et al. The c-erb-a protein is a high-affinity receptor for thyroid hormone. *Nature*. 1986;**324**:635–40.
 - 26 Laudet V, Begue A, Henry-duthoit C, Joubel A, Martin P, Stehelin D, et al. Genomic organization of the human thyroid hormone receptor α (c-erbA-1) gene. *Nucleic Acids Res*. 1991;**19**:1105–12.
 - 27 Laudet V, Hanni C, Coll J, Catzeflis F, Stehelin D. Evolution of the nuclear receptor gene superfamily. *EMBO J*. 1992;**11**:1003–13.
 - 28 Ishida T, Yamauchi K, Ishikawa K, Yamamoto T. Molecular cloning and characterization of the promoter region of the human c-erbA α gene. *Biochem Biophys Res Commun*. 1993;**191**:831–9.
 - 29 Vanacker JM, Bonnelye E, Delmarre C, Laudet V. Activation of the thyroid hormone receptor α gene promoter by the orphan nuclear receptor ERR α . *Oncogene*. 1998;**17**:2429–35.
 - 30 Van Der Flier LG, Clevers H. Stem cells, self-renewal, and differentiation in the intestinal epithelium. *Annu Rev Physiol*. 2009;**71**:241–60.
 - 31 Gehart H, Clevers H. Tales from the crypt: new insights into intestinal stem cells. *Nat Rev Gastroenterol Hepatol*. 2019;**16**(1):19–34.
 - 32 Freund JN, Domon-Dell C, Keding M, Duluc I. The Cdx-1 and Cdx-2 homeobox genes in the intestine. *Biochem Cell Biol*. 1998;**76**:957–69.
 - 33 Schepers A, Clevers H. Wnt signaling, stem cells, and cancer of the gastrointestinal tract. *Cold Spring Harb Perspect Biol*. 2012;**4**:a007989.
 - 34 Kulic I, Robertson G, Chang L, Baker JHE, Lockwood WW, Mok W, et al. Loss of the notch effector RBPJ promotes tumorigenesis. *J Exp Med*. 2015;**212**:37–52.
 - 35 Bonhomme C, Duluc I, Martin E, Chawengsaksophak K, Chenard MP, Keding M, et al. The Cdx2 homeobox gene has a tumour suppressor function in the distal colon in addition to a homeotic role during gut development. *Gut*. 2003;**52**:1465–71.
 - 36 Bray NL, Pimentel H, Melsted P, Pachter L. Near-optimal probabilistic RNA-seq quantification. *Nat Biotechnol*. 2016;**34**:525–7.
 - 37 Peignon G, Durand A, Cacheux W, Ayrault O, Terris B, Laurent-Puig P, et al. Complex interplay between β -catenin signalling and notch effectors in intestinal tumorigenesis. *Gut*. 2011;**60**:166–76.
 - 38 Hinoi T, Lucas PC, Kuick R, Hanash S, Cho KR, Fearon ER. CDX2 regulates liver intestine-cadherin expression in normal and malignant colon epithelium and intestinal metaplasia. *Gastroenterology*. 2002;**123**:1565–77.
 - 39 Rezza A, Skah S, Roche C, Nadjar J, Samarut J, Plateroti M. The overexpression of the putative gut stem cell marker Musashi-1 induces tumorigenesis through Wnt and notch activation. *J Cell Sci*. 2010;**123**:3256–65.
 - 40 Balbinot C, Vanier M, Armant O, Nair A, Penichon J, Soret C, et al. Fine-tuning and autoregulation of the intestinal determinant and tumor suppressor homeobox gene CDX2 by alternative splicing. *Cell Death Differ*. 2017;**24**:2173–86.
 - 41 Ying QL, Wray J, Nichols J, Battle-Morera L, Doble B, Woodgett J, et al. The ground state of embryonic stem cell self-renewal. *Nature*. 2008;**453**:519–23.
 - 42 Chen B, Dodge ME, Tang W, Lu J, Ma Z, Fan CW, et al. Small molecule-mediated disruption of Wnt-dependent signaling in tissue regeneration and cancer. *Nat Chem Biol*. 2009;**5**:100–7.
 - 43 Lu H, Cheng G, Hong F, Zhang L, Hu Y, Feng L. A novel 2-phenylamino-quinazoline-based compound expands the neural stem cell pool and promotes the hippocampal neurogenesis and the cognitive ability of adult mice. *Stem Cells*. 2018;**36**:1273–85.
 - 44 Pandya K, Meeke K, Clementz AG, Rogowski A, Roberts J, Miele L, et al. Targeting both notch and ErbB-2 signalling pathways is required for prevention of ErbB-2-positive breast tumour recurrence. *Br J Cancer*. 2011;**105**(6):796–806.
 - 45 Dovey HF, John V, Anderson JP, Chen LZ, Andrieu PDS, Fang LY, et al. Functional gamma-secretase inhibitors reduce beta-amyloid peptide levels in brain. *J Neurochem*. 2001;**76**:173–81.
 - 46 Shibata H, Toyama K, Shioya H, Ito M, Hirota M, Hasegawa S, et al. Rapid colorectal adenoma formation initiated by conditional targeting of the APC gene. *Science*. 1997;**278**:120–33.
 - 47 El Marjou F, Janssen KP, Chang BHJ, Li M, Hindie V, Chan L, et al. Tissue-specific and inducible Cre-mediated recombination in the gut epithelium. *Genesis*. 2004;**39**:186–93.
 - 48 Mlecnik B, Tosolini M, Kirilovsky A, Berger A, Bindea G, Meatchi T, et al. Histopathologic-based prognostic factors of colorectal cancers are associated with the state of the local immune reaction. *J Clin Oncol*. 2011;**29**:610–8.
 - 49 Galon J, Costes A, Sanchez-Cabo F, Kirilovsky A, Mlecnik B, Lagorce-Pagès C, et al. Type, density, and location of immune cells within human colorectal tumors predict clinical outcome. *Science*. 2006;**313**:1960–4.
 - 50 Vonlanthen J, Okoniewski MJ, Menigatti M, Cattaneo E, Pellegrini-Ochsner D, Haider R, et al. A comprehensive look at transcription factor gene expression changes in colorectal adenomas. *BMC Cancer*. 2014;**14**:46.

- 51 Bottomly D, Kyler SL, McWeeney SK, Yochum GS. Identification of β -catenin binding regions in colon cancer cells using ChIP-seq. *Nucleic Acids Res.* 2010;**38**:5735–45.
- 52 Cancer Genome Atlas Network. Comprehensive molecular characterization of human colon and rectal cancer. *Nature.* 2012;**487**:330–7.
- 53 Gayet J, Zhou XP, Duval A, Rolland S, Hoang JM, Cottu P, et al. Extensive characterization of genetic alterations in a series of human colorectal cancer cell lines. *Oncogene.* 2001;**20**:5025–32.
- 54 Berg KCG, Eide PW, Eilertsen IA, Johannessen B, Bruun J, Danielsen SA, et al. Multi-omics of 34 colorectal cancer cell lines – a resource for biomedical studies. *Mol Cancer.* 2017;**16**:116.
- 55 Ahmed D, Eide PW, Eilertsen IA, Danielsen SA, Eknæs M, Hektoen M, et al. Epigenetic and genetic features of 24 colon cancer cell lines. *Oncogenesis.* 2013;**2**:e71.
- 56 Lagziel S, Gottlieb E, Shlomi T. Mind your media. *Nat Metab.* 2020;**2**:1369–72.
- 57 Hasebe T, Fujimoto K, Kajita M, Ishizuya-Oka A. Thyroid hormone activates Wnt/ β -catenin signaling involved in adult epithelial development during intestinal remodeling in *Xenopus laevis*. *Cell Tissue Res.* 2016;**365**:309–18.
- 58 Najdi R, Syed A, Arce L, Theisen H, Ting JHT, Atcha F, et al. A Wnt kinase network alters nuclear localization of TCF-1 in colon cancer. *Oncogene.* 2009;**28**:4133–46.
- 59 Matano M, Date S, Shimokawa M, Takano A, Fujii M, Ohta Y, et al. Modeling colorectal cancer using CRISPR-Cas9-mediated engineering of human intestinal organoids. *Nat Med.* 2015;**21**:256–62.
- 60 Drost J, Van Jaarsveld RH, Ponsioen B, Zimmerlin C, Van Boxtel R, Buijs A, et al. Sequential cancer mutations in cultured human intestinal stem cells. *Nature.* 2015;**521**:43–7.
- 61 Merenda A, Fenderico N, Maurice MM. Wnt signaling in 3D: recent advances in the applications of intestinal organoids. *Trends Cell Biol.* 2020;**30**:60–73.
- 62 Wang CS, Lin KH, Hsu YC. Alterations of thyroid hormone receptor α gene: frequency and association with Nm23 protein expression and metastasis in gastric cancer. *Cancer Lett.* 2002;**175**:121–7.
- 63 Lin KH, Zhu XG, Shieh HY, Hsu HC, Chen ST, McPhie P, et al. Identification of naturally occurring dominant negative mutants of thyroid hormone $\alpha 1$ and $\beta 1$ receptors in a human hepatocellular carcinoma cell line. *Endocrinology.* 1996;**137**:4073–81.
- 64 Lin KH, Zhu XG, Hsu HC, Chen SL, Shieh HY, Chen ST, et al. Dominant negative activity of mutant thyroid hormone receptors from patients with hepatocellular carcinoma. *Endocrinology.* 1997;**138**:5308–15.
- 65 Stringer EJ, Duluc I, Saandi T, Davidson I, Bialecka M, Sato T, et al. Cdx2 determines the fate of postnatal intestinal endoderm. *Development.* 2012;**139**:465–74.
- 66 Pereira B, Sousa S, Barros R, Carreto L, Oliveira P, Oliveira C, et al. CDX2 regulation by the RNA-binding protein MEX3A: impact on intestinal differentiation and stemness. *Nucleic Acids Res.* 2013;**41**:3986–99.
- 67 San Roman AK, Tovaglieri A, Breault DT, Shivdasani RA. Distinct processes and transcriptional targets underlie CDX2 requirements in intestinal stem cells and differentiated villus cells. *Stem Cell Rep.* 2015;**5**:673–81.
- 68 Dalerba P, Sahoo D, Paik S, Guo X, Yothers G, Song N, et al. CDX2 as a prognostic biomarker in stage II and stage III colon cancer. *N Engl J Med.* 2016;**374**:211–22.
- 69 Balbinot C, Armant O, Elarouci N, Marisa L, Martin E, de Clara E, et al. The Cdx2 homeobox gene suppresses intestinal tumorigenesis through non-cell-autonomous mechanisms. *J Exp Med.* 2018;**215**:911–26.
- 70 Vu T, Straube J, Porter AH, Bywater M, Song A, Ling V, et al. Hematopoietic stem and progenitor cell-restricted Cdx2 expression induces transformation to myelodysplasia and acute leukemia. *Nat Commun.* 2020;**11**:3021.
- 71 Galland A, Gourain V, Habbas K, Güler Y, Martin E, Ebel C, et al. CDX2 expression in the hematopoietic lineage promotes leukemogenesis via TGF β inhibition. *Mol Oncol.* 2021;**15**:2318–29.
- 72 Hryniuk A, Grainger S, Savory JGA, Lohnes D. Cdx1 and Cdx2 function as tumor suppressors. *J Biol Chem.* 2014;**289**:33343–54.
- 73 Sakamoto N, Feng Y, Stolfi C, Kurosu Y, Green M, Lin J, et al. BRAFV600E cooperates with CDX2 inactivation to promote serrated colorectal tumorigenesis. *eLife.* 2017;**6**:e20331.
- 74 Salari K, Spulak ME, Cuff J, Forster AD, Giacomini CP, Huang S, et al. CDX2 is an amplified lineage-survival oncogene in colorectal cancer. *Proc Natl Acad Sci USA.* 2012;**109**:E3196–205.
- 75 Plateroti M, Chassande O, Fraichard A, Gauthier K, Freund JN, Samarut J, et al. Involvement of T3R α - and β -receptor subtypes in mediation of T3 functions during postnatal murine intestinal development. *Gastroenterology.* 1999;**116**:1367–78.
- 76 Plateroti M, Gauthier K, Domon-Dell C, Freund J-N, Samarut J, Chassande O. Functional interference between thyroid hormone receptor α (TR α) and natural truncated TR $\Delta\alpha$ isoforms in the control of intestine development. *Mol Cell Biol.* 2001;**21**:4761–72.
- 77 Barat S, Chen X, Bui KC, Bozko P, Götze J, Christgen M, et al. Gamma-secretase inhibitor IX (GSI) impairs concomitant activation of notch and wnt-beta-catenin pathways in CD441 gastric cancer stem cells. *Stem Cells Transl Med.* 2017;**6**:819–29.
- 78 Borggrefe T, Lauth M, Zwijssen A, Huylebroeck D, Oswald F, Giaimo BD. The notch intracellular domain integrates signals from Wnt, hedgehog, TGF β /BMP and hypoxia pathways. *Biochim Biophys Acta.* 2016;**1863**:303–13.

- 79 Krishnamurthy N, Kurzrock R. Targeting the Wnt/ β -catenin pathway in cancer: update on effectors and inhibitors. *Cancer Treat Rev.* 2018;**62**:50–60.
- 80 Collu GM, Hidalgo-Sastre A, Brennan K. Wnt-notch signalling crosstalk in development and disease. *Cell Mol Life Sci.* 2014;**71**:3553–67.
- 81 Ghandi M, Huang FW, Jané-Valbuena J, Kryukov GV, Lo CC, McDonald ER, et al. Next-generation characterization of the cancer cell line encyclopedia. *Nature.* 2019;**569**:503–8.
- 82 Sato T, Vries RG, Snippert HJ, van de Wetering M, Barker N, Stange DE, et al. Single Lgr5 stem cells build crypt-villus structures in vitro without a mesenchymal niche. *Nature.* 2009;**459**:262–5.
- 83 Silva A-L, Dawson SNN, Arends MJJ, Guttula K, Hall N, Cameron EAA, et al. Boosting Wnt activity during colorectal cancer progression through selective hypermethylation of Wnt signaling antagonists. *BMC Cancer.* 2014;**141**(14):1–10.
- 84 Hellevik AI, Åsvold BO, Bjørø T, Romundstad PR, Nilsen TIL, Vatten LJ. Thyroid function and cancer risk: a prospective population study. *Cancer Epidemiol Biomarkers Prev.* 2009;**18**:570–4.
- 85 Iishi H, Tatsuta M, Baba M, Okuda S, Taniguchi H. Enhancement by thyroxine of experimental carcinogenesis induced in rat colon by azoxymethane. *Int J Cancer.* 1992;**50**:974–6.
- 86 Illouz F, Laboureaux-Soares S, Dubois S, Rohmer V, Rodien P. Tyrosine kinase inhibitors and modifications of thyroid function tests: a review. *Eur J Endocrinol.* 2009;**160**:331–6.
- 87 Illouz F, Braun D, Briet C, Schweizer U, Rodien P. Endocrine side-effects of anti-cancer drugs: thyroid effects of tyrosine kinase inhibitors. *Eur J Endocrinol.* 2014;**171**:R91–9.
- 88 Fearon ER, Jones PA. Progressing toward a molecular description of colorectal cancer development. *FASEB J.* 1992;**6**:2783–90.

Supporting information

Additional supporting information may be found online in the Supporting Information section at the end of the article.

Fig. S1. Schematic representation of the *THRA*-luc constructs.

Fig. S2. Setup conditions for TR α 1 IHC in human tissue sections.

Fig. S3. Analysis of *THRA* expression in a human colorectal cancer cohort.

Fig. S4. Characteristics of individual cell lines at multiple molecular levels.

Fig. S5. Analyses of the pGL3-basic vector.

Fig. S6. Effect of the Wnt agonist and antagonist on endogenous TR α 1 expression.

Fig. S7. Effect of β -catenin/TCF transfection on endogenous TR α 1 expression.

Fig. S8. TopFlash activity is affected in the presence of TCF1-DN.

Fig. S9. Chromatin occupancy of β -catenin in the AXIN2 and MYC promoters.

Fig. S10. Complementary analysis on mouse enteroids.

Table S1. List of primers.

Table S2. List of antibodies.

Table S3. TMA analysis.